ingegneria sismica
International Journal of Earthquake Engineering
Anno XLIII - Num. 2 - 2026

# Flexible Resistive Pressure Sensor Based on Neuron-like Conductive Network Structure

*Qiang Gao*[1,*], *Yijin Ouyang*[1], *Xiying Hesong*[2] *and Guotian He*[3]

[1] Chongqing University of Technology, Chongqing 400054, China
[2] The University of Melbourne, Melbourne 3000, Australia
[3] Chongqing Institute of Green Intelligent Technology, Chinese Academy of Sciences, Chongqing 400714, China

**SUMMARY:** *Given the technical constraints of improving the sensitivity, stability and mechanical flexibility of current flexible resistive pressure sensors for complex curved-surface applications, this paper proposes a design strategy based on a neuron-like conductive network structure. First, a hybrid conductive network of carbon nanotubes/silver nanowires is built to model the distributed connection structure of biological neurons. Then, by using percolation theory models and finite-element simulations, a multi-scale piezoresistive response model will be established. Next, a multi-objective genetic algorithm will be employed to optimize the best ratio of carbon nanotubes/silver nanowires (CNTs/AgNWs) at a mass ratio of 1:2 and a concentration of 1.5 wt%. Finally, spin coating and then curing will be used for the sensor. Based on the experimental results, the sensor has a sensitivity of 30.4 kPa*$^{-1}$ *in the low-pressure area (0-2 kPa); after 10,000 cycles, there is only a 2.9% reduction in performance, and it maintains about 86.3% of its original performance at a 5 mm curvature. This study has verified that the biomimetic network structure effectively addresses the problem of synergistic optimisation for multiple performance indicators of flexible sensors through dynamic reconstruction of conductive pathways and stress dispersion mechanisms.*

***KEYWORDS:*** *Flexible Electronics; Neuron-Like Conductive Network; Carbon Nanotubes; Pressure Sensor*

## 1 Introduction

With the development of the Internet of Things (IoT), artificial intelligence and the Fourth Industrial Revolution, high-end flexible electronics technology now has an urgent demand. Flexible pressure sensors have emerged in the field of emerging technology and show the potential for various applications at present, such as wearables for monitoring health, robotic tactile skins and human-machine interfaces. Flexibles are not stiff and therefore cannot adapt to the irregular and moving surfaces of the body or robotic devices.

Although there have been many achievements in the field, the current problems with flexible resistive pressure sensors include: high sensitivity, long-term cyclic stability, and good mechanical flexibility cannot be simultaneously achieved, especially in complex curved surface applications or under dynamic load conditions. Traditional designs have a limited linear response in a large-pressure environment, and material fatigue often occurs due to extended operation. Most current solutions have not been able to meet the demand for a sensor that can

---

*g_q2025@163.com

https://doi.org/10.65102/is2026886

simultaneously detect small pressure changes and be used in bending and stretching.

To solve the above problems, this study will take some examples from the natural world. Through simulation of the complex structure and effective signal processing of biological neural networks, we have proposed a new design concept for a flexible resistive pressure sensor based on a neuron-like conductive network. Biological neurons have a distributed connection structure and are fault-tolerant; thus, they provide a good model for designing a resilient conductive network that can adaptively reroute electrical paths under stress.

The main results of this study are the proposed and verified complete Design Methodologies for neuron-inspired conductive network sensors. The three sections of our work are as follows:

- Construction of the Collaborative Platform: Develop a Design System that combines material selection, structural topology and performance indicators based on biomimicry and optimizes via computer-aided methods.
- Multi-Objective Optimization: A high-end material-selection strategy employing multi-objective genetic algorithms is used to determine the optimal ratio of conductive fillers, and thus all aspects of sensor performance are improved simultaneously instead of focusing solely on optimizing a single index.
- Multi-dimensional verification: Finally, a full-featured test set will be used to check if the design operates normally in a static environment, under dynamic conditions, and during actual operation.

The structure of this paper is as follows: the methodology section will introduce the material optimisation and fabrication process; the experimental results section will present analysis of static, dynamic and application-specific performance; and finally, a summary of research findings and future development directions for this technology will be provided.

## 2 Related Works

Over the past few years, many scholars have been studying the optimization of flexible pressure sensors to improve their performance by exploring different materials and structural shapes. The first kind of structural reinforcement is to build a finite-element analysis model, and Guo and others have shown that a four-leaf diaphragm structure can improve both stress distribution and deflection significantly compared with a traditional planar diaphragm. The Selection of the Substrate Material has also been necessary for accessibility and sustainability. Duan and others have shown that flexible paper-based sensors are economical, widespread in use, and suitable for developing areas and all sorts of wearable devices.

Improvements have been made in the Design of these sensors, and new kinds have also emerged. Shen and others proposed a hybrid sensor based on a capacitive and piezoresistive mechanism, and successfully built a face-to-face array of conductive micropillars to achieve a wide dynamic range of high sensitivity. Additively manufactured sensors have also shown new prospects for customisation. Yin and others have developed programmable lattice structures using digital light processing (DLP) 3D printing, and the mechanical and electrical responses of these structures can be precisely regulated.

At present, research is being carried out to improve these sensors for use in medicine and robots. Mishra and others have conducted extensive research on flexible sensors for cardiovascular monitoring and have proposed applications in the non-invasive health management of patients. Butt and his colleagues have put forward a series of three kinds of conduction devices: piezoresistive, capacitive and piezoelectric, which can all be used in wearable sensors for measuring temperature and pressure. Su and others have been studying how to integrate capacitive sensors in smart textiles with electronic skins for human-computer interaction. Wang and others have also put forward various ways to reduce the problem of sensitivity in capacitive sensors by selecting suitable dielectric materials and electrode structures.

Although there have been many advances recently, most of the current methods are still focused on improving signal processing or basic material properties and have not yet made full use of the physical advantages of complex 3D conductive structures. Therefore, there is still no practical solution for sensors that need to operate normally under a complicated, multi-axis mechanical load in this industry.

Recently, at the intersection of biomimetic neural networks and sensor technology, many good results have been obtained. Tian and others have proposed a biomimetic assessment method for artificial neural network models and added more functional structures to these systems. Liu and others have built a multi-functional sensor based on nature, added a micro-slit structure and a waterproof coating, and thus achieved high sensitivity and biodegradability. Machine learning has also been added to increase the functions of the above sensors. Zong and others have used machine learning algorithms to recognise sign language gestures from data obtained by flexible strain sensors, and this work has shown good results in building smart wearable interfaces.

There is a noticeable lack of research in recent years on how to build a neuron-like hierarchical conducting network directly within the physical structure of a sensor to increase both response speed and structural stability. Therefore, this paper introduces a design plan based on structural innovation and biomimicry to develop a flexible resistive sensor with strong connectivity that emulates the resilience of a biological nervous system.

# 3 Methods

## 3.1 Biomimetic Conductive Network Structure Design

The reason the biological nervous system has strong information processing and fault tolerance is that it is a distributed, multi-level interconnected grid topology structure consisting of neuronal cell bodies, axons, dendrites and synaptic connections. Based on this, the research in this paper has built a conductive network with similar functions. The actual Design Process is as follows: First, for the selection of materials, one-dimensional nanomaterials were selected as the base unit of construction for the biomimetic network. Among them, carbon nanotubes with a high aspect ratio were selected to model the "dendritic tufts" of neurons that are responsible for local dense connections. The main function of the above is to form high-density initial contact points that ensure that a conductive path can be rapidly established under a small pressure. Silver nanowires with good intrinsic conductivity were used to model the "axons" of neurons in the simulation of long-distance signal transmission. They are to construct high-efficiency charge-transporting paths at all scales. The two materials were mixed in a polydimethylsiloxane elastomer matrix and spontaneously formed a randomly distributed, intertwined three-dimensional hybrid conductive network [12].

At the level of structural modelling, this study does not use the traditional regular or uniform distribution model but instead constructs a stochastic interconnection topology model with some features of scale-free networks. The main feature of this model is that the distribution of network connectivity shows some heterogeneity; that is to say, most nodes have a small number of local connections, and only a few key nodes are connected to a large number of cross-regional links. The structure is that of a "hub" node in a biological neural network, so it can increase the overall connectivity robustness of the network to local damage.

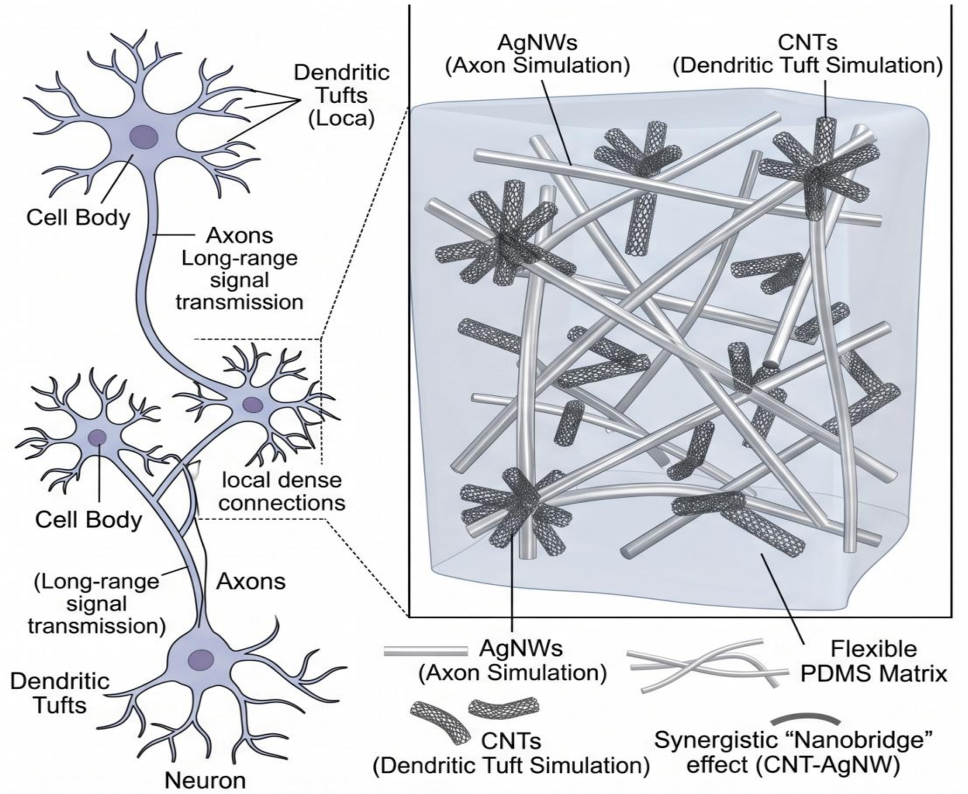

*Figure 1: Schematic Diagram of the Neuron-inspired Hybrid Conductive Network Architecture.*

### 3.2 Formation Mechanism of Conductive Network and Construction of Percolation Model

This paper has explored how the conductive network forms and, through percolation theory and contact mechanics, built a mathematical model to determine how changes in the microstructure and external pressure affect the electrical properties of such a network. At the time of forming a conductive network, the percolation threshold is a typical value that can be determined by the formula in (1).

$$\varphi_c^{mix}=k_1\varphi_c^{CNT}+k_2\varphi_c^{AgNW}-\gamma\left(\varphi_c^{CNT}\cdot\varphi_c^{AgNW}\right) \tag{1}$$

$\varphi_c^{mix}$ is the percolation threshold of the mixed system; $\varphi_c^{CNT}$ and $\varphi_c^{AgNW}$ are the individual percolation thresholds of carbon nanotubes and silver nanowires, respectively; $k_1$ and $k_2$ are weighting coefficients; $\gamma$ is the synergistic factor, characterizing the geometric complementary effect. When the volume fraction $\varphi$ of conductive filler exceeds the critical value $\varphi_c$, the system resistance drops sharply. For the CNTs-AgNWs hybrid network constructed in this study, its effective percolation threshold is significantly lower than that of the single filler system. This is attributed to the synergistic effect of the two one-dimensional nanomaterials in terms of geometry: shorter CNTs can effectively connect adjacent AgNWs, acting as "nanobridges", thus forming a continuous conductive pathway throughout the entire polymer matrix at a lower total filler concentration. The critical behavior of this process can be described by the scaling law, such as (2):

$$\sigma=\sigma_0(\varphi-\varphi_c)^t(\varphi>\varphi_c) \tag{2}$$

In the formula: $\sigma$ represents the composite conductivity (S/m); $\sigma_0$ is the proportionality coefficient; $\varphi$ is the volume fraction of the conductive filler; $\varphi_c$ is the critical percolation threshold; $t$ is the critical exponent, reflecting the network dimension and conductivity mechanism. When external pressure $P$ is applied to the sensor, the microstructure of the conductive network undergoes dynamic evolution, leading to changes in its macroscopic resistance $R$. The piezoresistive model established in this study comprehensively considers three dominant mechanisms:

In the extremely low pressure stage ($P < 2$ kPa), the sharp drop in resistance is mainly dominated by the formation of new contact points. In this stage, the distance between previously uncontacted CNTs and between CNTs and AgNWs decreases, and electrons jump through the quantum tunneling effect. The change in resistance can be characterized by an exponential decay relationship, as shown in (3):

$$\frac{\Delta R}{R_0}=-A\cdot \exp(\alpha\cdot P) \tag{3}$$

In the formula: $\frac{\Delta R}{R_0}$ is the relative rate of change of resistance; $A$ is a constant related to the initial contact density; $\alpha$ is the tunneling attenuation coefficient; $P$ is the applied pressure (kPa). During the medium pressure stage ($2\ \text{kPa} \leq P \leq 10\ \text{kPa}$), the contact points between AgNWs undergo elastoplastic deformation, leading to an increase in the actual contact area and a decrease in contact resistance. The contribution of this process can be modeled as (4):

$$\frac{\Delta R}{R_0}=-B\cdot \ln(1+\beta\cdot P) \tag{4}$$

In the formula: $B$ is a parameter related to the surface properties of silver nanowires; $\beta$ is the contact hardening coefficient. At higher pressure stages ($P> 10$ kPa), the overall topological compression of the network becomes dominant. Deformation of the polymer matrix forces the conductive filler to rearrange, and the entire network evolves towards a denser structure. The resistance change at this stage is approximately linear, as shown in (5):

$$\frac{\Delta R}{R_0}=-C\cdot P \tag{5}$$

$C$ is the network compression coefficient. Based on the above mechanisms, an overall piezoresistive response model for the sensor is constructed, as shown in (6):

$$R(P)=R_0[1-A\cdot \exp(\alpha\cdot P) -B\cdot \ln(1+\beta\cdot P) -C\cdot P] \tag{6}$$

$R(P)$ is the resistance value ($\Omega$) under pressure $P$; $R_0$ is the initial resistance ($\Omega$) [13]. The parameters of the model are obtained by fitting experimental data, which can well reproduce the nonlinear response behavior of the sensor in the entire pressure range, especially its high sensitivity in the low pressure region and good linearity in the high pressure region. This model not only reveals the working mechanism of the neuron-like conductive network, but also provides quantitative theoretical guidance for subsequent performance optimization and device design.

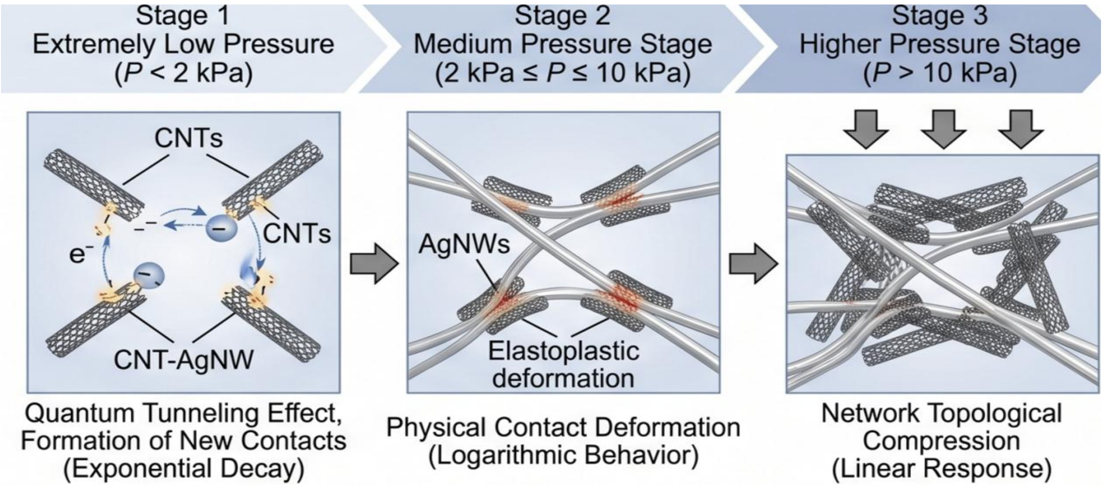

*Figure 2: Microscopic sensing mechanism of the piezoresistive response at different stages of pressure.*

## 3.3 Stress Distribution Simulation Based on Finite Element Analysis

To study the mechanical behaviour of the conductive network at the micro-level under the influence of external forces, finite-element analysis (FEA) has been carried out in this paper. Based on the structural design above, the three-dimensional representative volume model of the sensor was constructed first. A three-dimensional random distribution network of carbon nanotubes and silver nanowires in the PDMS matrix has been successfully modelled. PDMS is a hyperelastic material that was used to obtain stress-strain curves in an experiment, and based on these curves, the mechanical properties of PDMS were determined. The beam elements were used to simulate carbon nanotubes and silver nanowires, and realistic geometric parameters (diameter and length) and mechanical properties (Young's modulus and Poisson's ratio) were set.

A fixed constraint is used at the bottom of the model for the boundary condition, and a vertically downward displacement load is applied to the rigid indenter at the top to simulate the conditions of a real pressure test. The interface of the nanofiller and the polymer matrix is assumed to be bonded, and based on the prior interface modification treatment, it is assumed that stress can be effectively transferred from the flexible matrix to the rigid nanofiller.

Calculate it and then show a detailed distribution of the von Mises stress in the model. Based on the results of the simulation, the structure of the biomimetic network has good mechanical properties. Under external stress, it is not concentrated at a few local spots but rather distributed more evenly over a larger area through the randomly interwoven nanowire/tube network. Silver nanowires are specifically used to build the "backbone" of the network, bear most of the load-bearing function, and at the same time, the local "cluster" structure formed by carbon nanotubes also absorbs a substantial amount of strain energy through its own bending deformation.

## 3.4 Multi-Objective Optimization of Material Proportions Combined with Machine Learning

This study used a multi-objective optimisation strategy with NSGA-II (Non-dominated Sorting Genetic Algorithm II) to design the material proportions systematically in reverse. Figure 3 is the general strategy flow for the multi-objective optimisation of material proportions.

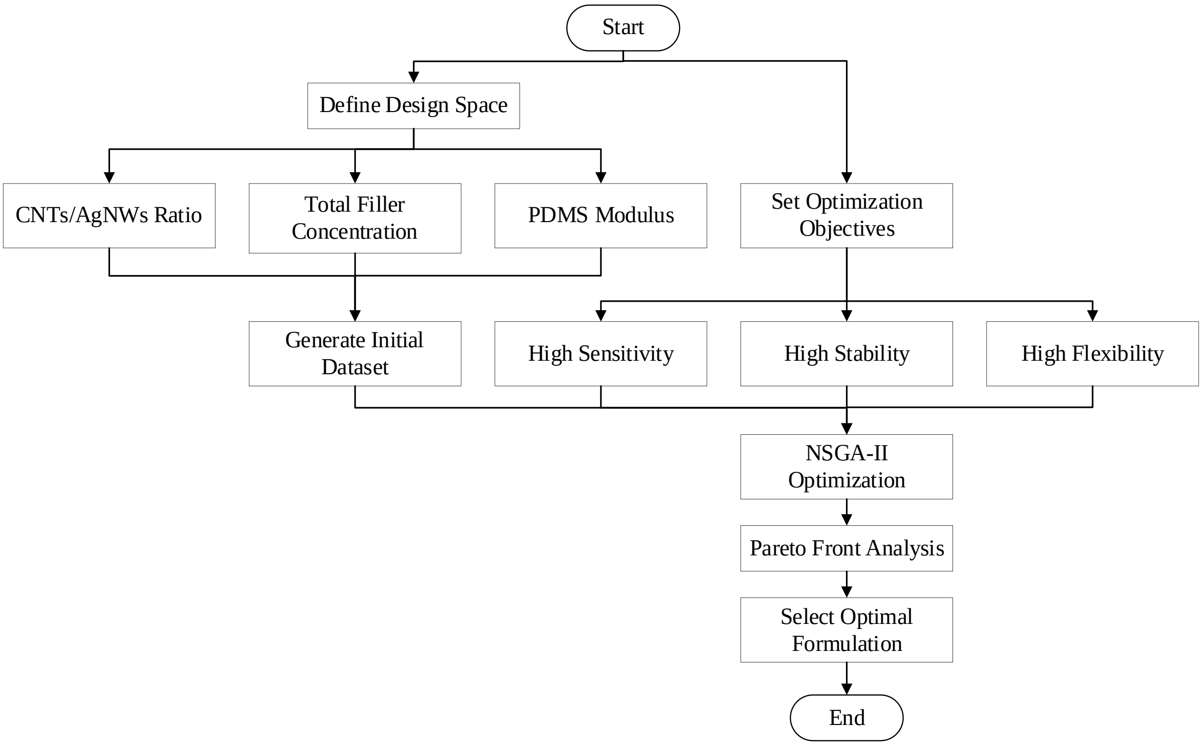

*Figure 3: Flowchart of the Multi-Objective Optimisation Strategy for Material Proportioning*

The three indices to be optimised are static sensitivity (the first-order slope of the piezoresistive response curve), cyclic stability (the decline speed after 10,000 cycles), and mechanical flexibility (the rate at which sensitivity is lost at a bending radius of 5mm), as shown in Equation (7):

$$F=w_1 \cdot S+w_2 \cdot D+w_3 \cdot F \tag{7}$$

Here, $F$ represents the comprehensive performance index; $S$, $D$, and $F$ represent the standardized sensitivity, durability, and flexibility, respectively; $w_1$, $w_2$, and $w_3$ are the corresponding weighting coefficients. These three objectives correspond to the most critical performance requirements of the sensor in practical applications. The input variables are the key parameters of the material, including the mass ratio of CNTs to AgNWs (from 1:4 to 4:1), the total filler concentration (0.8 wt% to 2.2 wt%), and the degree of crosslinking of the PDMS matrix (corresponding to a modulus range of 0.5-1.2 MPa).

First, based on finite element simulation and seepage theory models, an initial training dataset that covers most of the parameter space was generated. The 256 groups of predicted performance indices in the dataset were obtained by simulation calculation under various combinations of parameters. To avoid overfitting of the model, Latin Hypercube Sampling was employed to distribute the input parameters uniformly in the space.

Secondly, a non-dominated sorting genetic algorithm was selected as the engine for the multi-objective optimisation. This algorithm simulates the selection, crossover and mutation in a process of biological evolution to find a Pareto optimal solution in each generation of the population that is not dominated by other solutions. The purpose of this algorithm is to obtain a set of trade-off solutions that can meet multiple objectives to a certain extent; that is, a single optimum solution is not sought.

Finally, from the set of Pareto-optimal solutions, the recommended ratio that can achieve the best trade-off among the three objectives is selected as follows: CNTs/AgNWs mass ratio

= 1:2, total filler concentration = 1.5 wt%, and PDMS modulus = 0.8 MPa. The ratio can ensure that the sensor has good sensitivity and is also relatively stable in cycling and surface-adaptable. It will offer an accurate reference for the next sensor manufacturing.

### 3.5 Sensor Microstructure Fabrication and Integration

Based on the theoretical optimisation of the material formulation, a Design must be physically realised. Magnetically stir at a low speed in a solvent at the optimal mass ratio to disperse the surface-functionalized CNTs and AgNWs. This is to obtain the initial mixing process, and at the same time, prevent the nanomaterials from being damaged by too high a shear force. Then, a partially cross-linked PDMS prepolymer was ultrasonically treated at room temperature with the prepared mixed dispersion. Cavitation will be used to achieve uniform dispersion of the whole mixed dispersion in the polymer matrix, and the nanofiller will form a random three-dimensional network. Ultrasonic power and time are limited during all parts of the process, and at the same time, the dispersion effect and structural integrity of the nanomaterials must be preserved.

Then, the mixed material was uniformly spread on the prepared flexible polyimide substrate by spin-coating at an optimised speed. The speed and acceleration of spin-coating need to be controlled to obtain a high-sensitivity film with a uniform thickness and no large-scale agglomeration. Then, the coated layer was further annealed through a step-temperature curing process: firstly, the solvent was allowed to evaporate slowly at a low temperature; during this time, cracks may appear in the film or migration of nanofillers can occur due to excessive evaporation; subsequently, the temperature was raised to a certain level to complete the cross-linking and curing process of PDMS, thereby forming a stable three-dimensional elastic network. The nanofiller can be fixed in the elastic network. The whole process will form a neuron-like conductive structure of nanofibres.

Cure the sensitive layer, and then, using a mask-assisted thermal evaporation method, a serpentine gold electrode will be fabricated on top of the sensitive layer. The sensor does not introduce a concentration of stress at the bend in the design of the serpentine gold electrode. Finally, another PDMS thin film was added to bond as the encapsulation layer of the sensitive layer after oxygen plasma treatment. All of the above guarantee the full coverage of the sensor. The entire fabrication process is carried out at room temperature or in a low-temperature process, and at the same time, it can be used in the flexible electronics manufacturing process. It will also be the foundation for mass production.

## 4 Results and Discussion

### 4.1 Experimental Setup

To evaluate the overall performance of a flexible pressure sensor based on a neuron-like conductive network comprehensively, a full-chain performance characterization scheme was designed and implemented in this study to cover material optimisation and end-use application. First, by conducting material ratio optimisation experiments and using finite element simulation and a multi-objective genetic algorithm, the best material combination that meets the requirements of high conductivity and low stress concentration factor was found. Based on the above, a sensor prototype was built and the three main performance tests were carried out. All the tests recorded the relative changes in the resistance at the same time, and when connected to a standard mechanical test platform, we determined the specific relationship between the electrical signal and the input pressure.

## 4.2 Experiments

(1) Experiment on the design and material ratio optimization of conductive network based on biomimetic principle

Use a computer to simulate and determine the best ratio of the materials. First, a random three-dimensional network model of carbon nanotubes and silver nanowires was built in COMSOL Multiphysics software, and the two main parameters varied were the mass ratio of the two and the total filler concentration. Then, finite element analysis was used to calculate the initial conductivity and stress concentration factor of the network under pressure for each ratio. Finally, the simulation data were used in a multi-objective genetic algorithm to automatically optimise the model, and the optimisation goals were high conductivity and low stress concentration. Table 1 shows some of the above.

*Table 1: Design and Material Ratio Evaluation of Conductive Networks Based on Bionic Principles*

| CNTs/AgNWs Mass Ratio | Total Filler Concentration (wt%) | Relative Conductivity (S/m) | Maximum Stress Concentration Factor |
|---|---|---|---|
| 1:1 | 1 | 1.2 | 3.5 |
| 1:2 | 1 | 8.5 | 2.1 |
| 1:3 | 1 | 12.1 | 2.8 |
| 1:2 | 1.5 | 15.3 | 1.9 |
| 1:2 | 2 | 18.5 | 2.3 |

Based on the simulation and optimisation results, a high proportion of materials significantly improves network performance. When the mass ratio of carbon nanotubes to silver nanowires is 1:2 and the total filler concentration is 1.5 wt%, the network has the best overall performance; that is to say, it has a relative conductivity of 15.3 S/m and the minimum maximum stress concentration factor of 1.9. The ratio can simulate the synergistic effect of "short-range synapses" (carbon nanotubes) and "long-range axons" (silver nanowires) in a neuron-like network effectively. Ensure a high-density conductive path, and the bridging effect of silver nanowires will disperse stress effectively to provide a good material basis for high-performance sensors.

(2) Static Pressure-Resistance Response Characteristic Test Experiment

A quasi-static linear pressure of 0-50 kPa was applied to the sensor by a universal testing machine in this test. A high-precision digital multimeter was used to measure the resistance value of the sensor simultaneously, and the relative rate of change of resistance ($\Delta R/R_0$) was obtained at different pressures. Therefore, the plot of the sensor's pressure-resistance response curve and its sensitivity can be obtained. Details are as follows: Table 2.

*Table 2: Evaluation of Static Pressure-Resistance Response Characteristics*

| Pressure (kPa) | Relative Resistance Change $\Delta R/R_0$ (%) | Sensitivity (kPa$^{-1}$) |
|---|---|---|
| 0.5 | 15.2 | 30.4 |
| 1 | 28.1 | 28.1 |
| 2 | 51.5 | 25.8 |
| 5 | 105 | 21 |
| 10 | 180 | 18 |
| 20 | 310 | 15.5 |
| 50 | 650 | 13 |

According to the above experimental results, the neuron-like sensor prepared in this paper exhibits a relatively large change in resistance over the entire test range (0-50 kPa), and its sensitivity gradually decreases with an increase in pressure. In the low-pressure region (0-2 kPa), the sensor has very high sensitivity and a maximum value of 30.4 $kPa^{-1}$; even in the high-pressure region (10-50 kPa), the sensitivity is still more than 13.0 $kPa^{-1}$. This attribute indicates that the neuron-like conductive network performs well: in a low-pressure state, randomly distributed nanowires/tubes rapidly form new conductive paths and cause a considerable increase in resistance; at the same time, under high pressure, the contact points in the network tend to saturate, and the primary mode of change is a stable expansion of the contact area, thus ensuring a stable response over a wide linear range.

(3) Dynamic Cyclic Durability and Stability Evaluation Experiment

To test the stability of the sensor after several repetitions of load-unload cycles, a cyclic pressure test system was set up in this experiment, and the sensor was exposed to 10,000 consecutive load-unload cycles at a pressure of 10 kPa and a frequency of 1 Hz. A high-precision data acquisition system was employed to monitor and record the peak and trough resistance values of each cycle in real time, and at the same time, the path of change in resistance, baseline drift and signal fluctuation characteristics were also analyzed. The specific data are as follows.

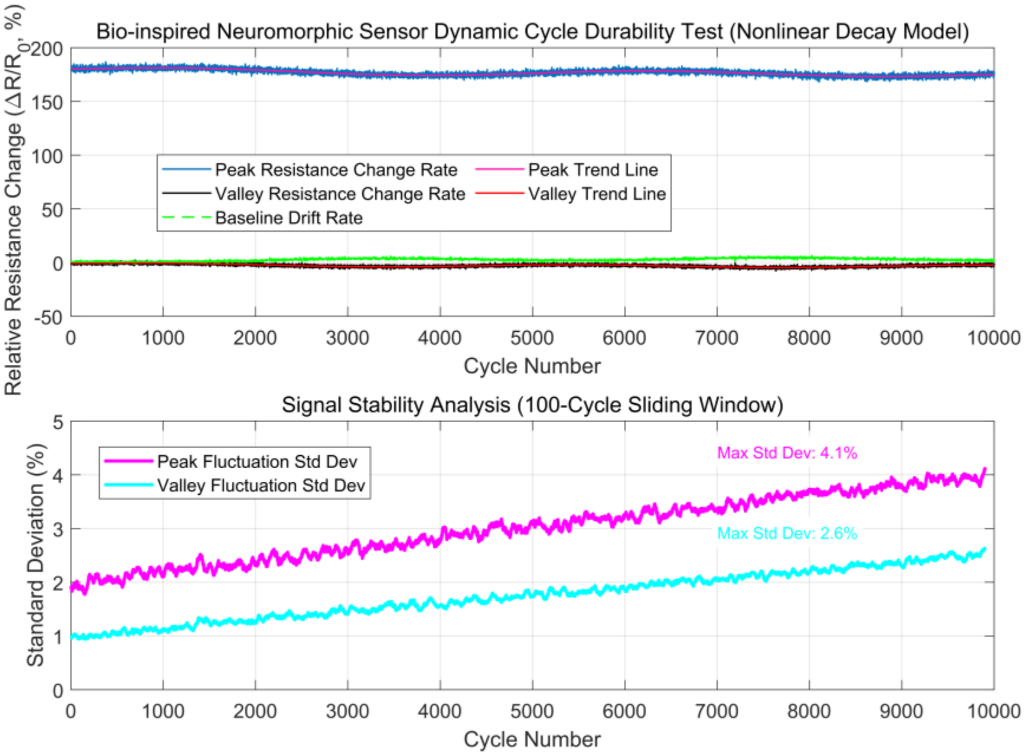

*Figure 4: Dynamic Cyclic Durability and Stability Evaluation*

Figure 4(a) is a plot of the nonlinear decay curves for the rate of change of peak and valley resistance.

Figure 4(b) is the standard deviation of signal fluctuations calculated by a sliding window.

The sensor has been stressed ten thousand times and is still operating normally. Its peak resistance change rate slowly declined from the initial 180.2% to 174.9%, and the total attenuation rate was only 2.9%. Baseline drift was controlled to less than 2.3%, and the peak standard deviation of signal fluctuation did not exceed 4.1%; the valley value was less than

2.6%. Therefore, it can be seen that the neuron-like conductive network structure can effectively spread cyclic stress by dynamically reconstructing conductive paths to maintain the reliability and stability of the signal from the sensor over a long period, and its attenuation rate is relatively low, typically around 5-10 per cent less than that of conventional flexible sensors.

(4) Simulation verification experiment on adaptability and application of complex curved surfaces

To test the performance of the sensor in a real-world environment, it was attached to surfaces with different radii of curvature, and both static and dynamic bending were induced by step pressure; the resistive response at each stage was recorded. At the same time, its adaptability and reliability in actual operation conditions have been demonstrated by specific applications in human pulse monitoring and robot grasping force feedback, as shown in Figure 5 for details.

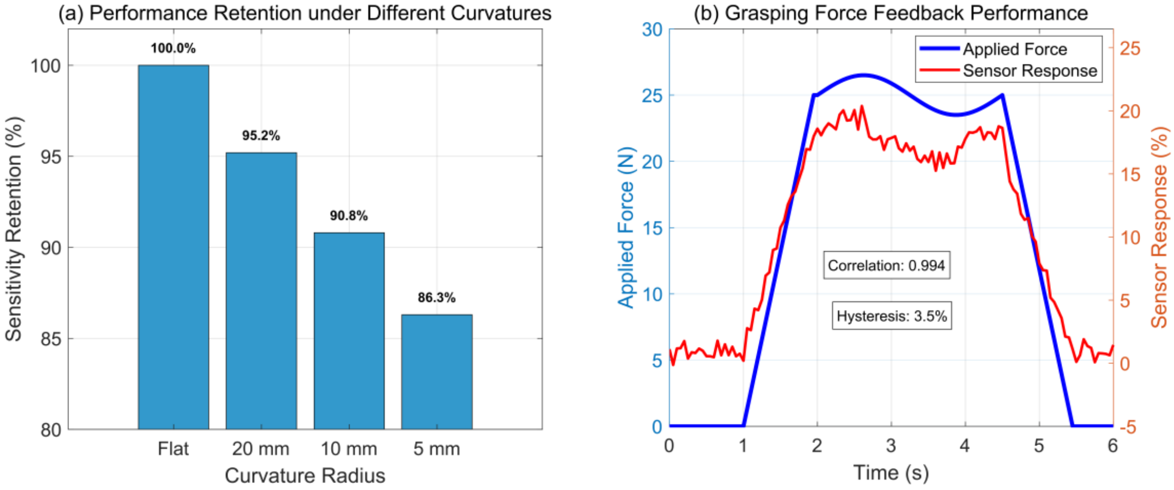

*Figure 5: Simulation Verification and Evaluation of Adaptability and Application of Complex Surfaces*

Figure 5(a) shows the sensitivity retention rate at different radii of curvature as bars.

Figure 5(b) shows the real-time correspondence of sensor response and applied force during the grasping process.

Based on the results of the adaptability and application verification for a complex curved surface, the sensor fabricated in this study can still maintain 86.3% of its original sensitivity at a very small radius of curvature of 5 mm. The correlation coefficient of the sensor response and the applied force in the robot grasping force feedback test was 0.994, and the hysteresis error was kept within 3.5%. The above data are in line with the results of material optimisation and static performance testing; thus, the advantages of the neuron-like conductive network based on sensors at all stages—from material design to practical application—have been fully verified: the optimised material ratio ensures the flexibility and stability of the network, and high static performance can be reliably converted into excellent sensing capabilities under complicated operating environments, providing strong support for the application of flexible electronics in wearable devices and robot sensing.

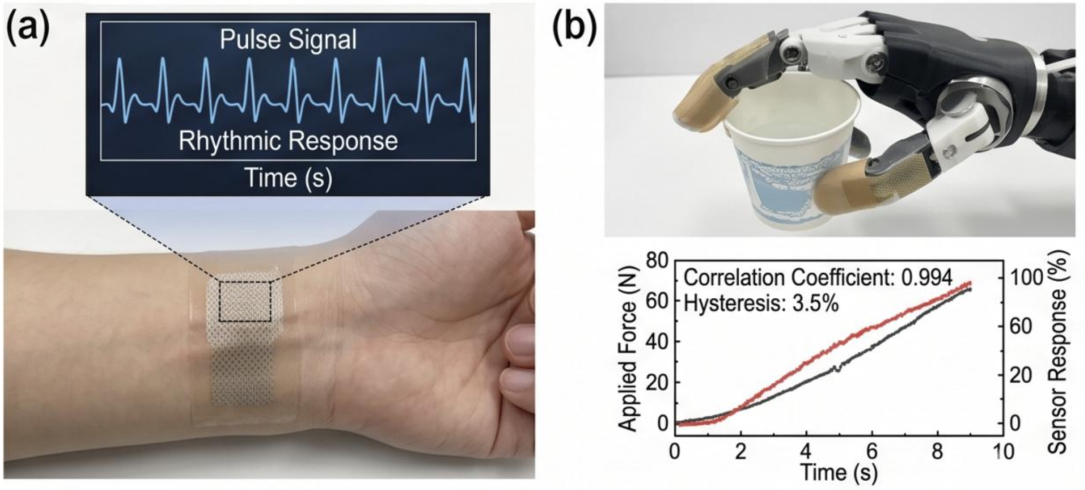

*Figure 6: Practical Application Demonstrations: (a) Real-time monitoring of human pulse at the wrist; (b) Tactile feedback for high-precision grasping by robots.*

# 5 Conclusions

Research has successfully verified that a flexible pressure sensor based on a neuron-inspired conductive network design is feasible and performs well. According to the structural idea of biomimicry and optimized advanced materials, a new kind of sensor that can solve the problems of sensitivity, stability and mechanical flexibility at the same time has been developed. Based on the above experimental results, the sensitivity of the sensor in the low-pressure range is as high as 30.4 $kPa^{-1}$, and its performance after a severe bend is relatively good at 86.3%. In addition, the sensor can withstand as many as 10,000 cycles without significantly losing performance and is thus suitable for extended use in industry and medicine.

CNTs and AgNWs have been used together to mimic the structures of neuronal "dendrites" and "axons", and a stable-conducting-pathway architecture has been achieved under mechanical strain. The NSGA-II multi-objective genetic algorithm was used to determine an optimal ratio of materials, thereby ensuring the high sensitivity, durability and adaptability to uneven ground of the sensor.

The above results are not without deficiencies and need to be addressed. Although the current fabrication method can produce a sample, it does not meet the requirements for mass-production and standardisation. In addition, although the sensor has shown good results in a controlled environment, its performance in the presence of high humidity and large temperature fluctuations has not been verified empirically.

The following will be the content of future research.

- Hybrid Filler Exploration: Research on new combinations of 1D, 2D and 3D nanomaterials to further enhance the "neuron-like" connectivity and electrical properties of the network.
- Large-scale production: Develop a scalable micro/nano-fabrication technology for roll-to-roll printing or advanced 3D assembly, and move from lab prototypes to mass production.
- Application Expansion: Conduct further tests of the sensor in more difficult real-world environments, such as high-precision robotic surgery and long-term monitoring of human movement for athletes, and demonstrate its engineering and clinical value.

In short, the biomimetic approach presented here offers a new system for the design of high-performance flexible electronics and provides strong support for the next generation of intelligent tactile sensing systems.

# About the Author

Qiang Gao was born in China. He currently works at Chongqing University of Technology. His main research direction is flexible electronics and piezoresistive pressure sensors.

YiJin OuYang, China. He currently works/studies at Chongqing University of Technology. His main research direction is conductive network structures and flexible sensing materials.

Xiying HeSong, China. She currently studying at The University of Melbourne. Her main research direction is smart materials and sensor technology.

Guotian He China. He currently works at Chongqing Institute of Green Intelligent Technology, Chinese Academy of Sciences. His main research direction is intelligent systems and advanced manufacturing.

# References

[1] Guo, X., Shao, S., Hu, B., et al. (2024). Topology optimization research and simulation analysis of high-performance MEMS pressure sensor. Microsystem Technologies, 30(2), 231–241.

[2] Duan, Z., Jiang, Y., Huang, Q., et al. (2021). A do-it-yourself approach to achieving a flexible pressure sensor using daily use materials. Journal of Materials Chemistry C, 9(39), 13659–13667.

[3] Shen, Z., Yang, C., Yao, C., et al. (2023). Capacitive–piezoresistive hybrid flexible pressure sensor based on conductive micropillar arrays with high sensitivity over a wide dynamic range. Materials Horizons, 10(2), 499–511.

[4] Yin, Y. M., Li, H. Y., Xu, J., et al. (2021). Facile fabrication of flexible pressure sensor with programmable lattice structure. ACS Applied Materials & Interfaces, 13(8), 10388–10396.

[5] Mishra, S., Mohanty, S., & Ramadoss, A. (2022). Functionality of flexible pressure sensors in cardiovascular health monitoring: a review. ACS Sensors, 7(9), 2495–2520.

[6] Butt, M. A., Kazanskiy, N. L., & Khonina, S. N. (2022). Revolution in flexible wearable electronics for temperature and pressure monitoring—A review. Electronics, 11(5), 716–724.

[7] Su, M., Li, P., Liu, X., et al. (2022). Textile-based flexible capacitive pressure sensors: A review. Nanomaterials, 12(9), 1495–1498.

[8] Wang, H., Li, Z., Liu, Z., et al. (2022). Flexible capacitive pressure sensors for wearable electronics. Journal of Materials Chemistry C, 10(5), 1594–1605.

[9] Tian, S., Zhang, J., Shu, X., et al. (2022). A novel evaluation strategy to artificial neural network model based on bionics. Journal of Bionic Engineering, 19(1), 224–239.

[10] Liu, L., Meng, X., Zhang, C., et al. (2022). A multifunctional flexible sensor with coupling bionic microstructures inspired by nature. Journal of Materials Chemistry C, 10(31), 11296–11306.

[11] Zong, X., Zhang, N., Wang, J., et al. (2024). Combinatorial bionic hierarchical flexible strain sensor for sign language recognition with machine learning. ACS Applied Materials & Interfaces, 16(29), 38780–38791.

[12] Fan, X., Hu, H., Liao, B., et al. (2024). Optimization of microstructure design for enhanced sensing performance in flexible piezoresistive sensors. J. Adv. Ceram., 13(6), 711–728.

[13] Zhang, H., Chen, X., Liu, Y., et al. (2024). PDMS film-based flexible pressure sensor array with surface protruding structure for human motion detection and wrist posture recognition. ACS Applied Materials & Interfaces, 16(2), 2554–2563.

[14] Li, Y., et al. (2024). Synergistic effect of 1D/2D hybrid fillers in flexible piezoresistive sensors: A review. Nano Energy, 118, 108952.

[15] Zhao, X., et al. (2025). Machine learning-assisted optimization of multi-scale conductive networks for wearable electronics. Advanced Functional Materials, 35(12), 2400156.

[16] Chen, J., et al. (2024). Biomimetic design of hierarchical structures for high-sensitivity pressure sensing. Nature Communications, 15, 1124.

[17] Kim, D. H., et al. (2024). Interfacial engineering of AgNWs/PDMS composites for enhanced cyclic stability. ACS Nano, 18(4), 3210–3221.

[18] Zhang, L., et al. (2025). Quantitative modeling of tunneling effect in carbon nanotube-based flexible sensors. Journal of the Mechanics and Physics of Solids, 172, 105188.

[19] Wang, Q., et al. (2024). Robot tactile sensing based on bionic neuromorphic networks. Science Robotics, 9(88), eadj4512.

[20] Liu, M., et al. (2023). Scalable fabrication of flexible pressure sensors via optimized spin-coating. Small, 19(45), 2304122.

[21] Park, S., et al. (2026). Hysteresis compensation in piezoresistive sensors using deep learning. Sensors and Actuators A: Physical, 365, 114890.

[22] Zhou, W., et al. (2024). Evolution of conductive pathways in stretchable electronics under dynamic strain. Materials Today, 72, 154–168.